



**HAL**  
open science

## The Influence of Bounding Plates on Species Separation in a Vertical Thermogravitational Column

Abdelkader Mojtabi, Pierre Costeseque, Bafétigué Ouattara, Marie Catherine Charrier-Mojtabi, D. Andrew S. Rees

► **To cite this version:**

Abdelkader Mojtabi, Pierre Costeseque, Bafétigué Ouattara, Marie Catherine Charrier-Mojtabi, D. Andrew S. Rees. The Influence of Bounding Plates on Species Separation in a Vertical Thermogravitational Column. *Physics*, 2022, 4 (1), pp.51-65. 10.3390/physics4010005 . hal-04120331

**HAL Id: hal-04120331**

**<https://hal.science/hal-04120331>**

Submitted on 7 Jun 2023

**HAL** is a multi-disciplinary open access archive for the deposit and dissemination of scientific research documents, whether they are published or not. The documents may come from teaching and research institutions in France or abroad, or from public or private research centers.


L'archive ouverte pluridisciplinaire **HAL**, est destinée au dépôt et à la diffusion de documents scientifiques de niveau recherche, publiés ou non, émanant des établissements d'enseignement et de recherche français ou étrangers, des laboratoires publics ou privés.



Distributed under a Creative Commons Attribution 4.0 International License

## Article

# The Influence of Bounding Plates on Species Separation in a Vertical Thermogravitational Column

Abdelkader Mojtabi <sup>1,\*</sup> , Pierre Costesque <sup>1</sup>, Bafétigué Ouattara <sup>2</sup>, Marie-Catherine Charrier-Mojtabi <sup>1</sup> and D. Andrew S. Rees <sup>3</sup>

<sup>1</sup> I.M.F.T., UMR CNRS/INP/UPS, Université de Toulouse, 31400 Toulouse, France;

pierre.costesque@toulouse-inp.fr (P.C.); marie-catherine.mojtabi@univ-tlse3.fr (M.-C.C.-M.)

<sup>2</sup> UFR SFA, Université Nangui Abrogoua, Abidjan 02, Côte d'Ivoire; ouattarabafetigue@yahoo.fr

<sup>3</sup> Department of Mechanical Engineering, University of Bath, Bath BA2 7AY, UK; ensdasr@bath.ac.uk

\* Correspondence: abdelkader.mojtabi@toulouse-inp.fr

**Abstract:** In this paper, an analytical and numerical analysis of the species separation in a binary mixture is performed. The main objective is to study the influence of the thickness and the nature of the bounding plates of the thermogravitational column (TGC) on species separation. The theory of Furry, Jones and Onsager is extended to the cases where bounding conducting walls enclose the TGC. The governing 2-dimensional equations are solved numerically using COMSOL Multiphysics software. A good agreement is found between the analytical and the numerical results. It is shown that the determination of the thermal diffusion coefficient,  $D_T$ , from the measurement of the vertical mass fraction gradient of binary solutions, does not depend on the temperature difference imposed on the vertical column either on the outer walls of the cavity or on the inner walls in contact with the binary solutions. However, it is found that this result is no longer valid in the case of a binary gas. To our knowledge, in all earlier studies, dealing with the measurement of Soret coefficients in binary fluids, the nature and the thickness of the bounding walls were not considered.

**Keywords:** convection; Soret effect; thermogravitational columns; species separation



**Citation:** Mojtabi, A.; Costesque, P.; Ouattara, B.; Charrier-Mojtabi, M.-C.; Rees, D.A.S. The Influence of Bounding Plates on Species Separation in a Vertical Thermogravitational Column. *Physics* **2022**, *4*, 51–65. <https://doi.org/10.3390/physics4010005>

Received: 9 December 2021

Accepted: 4 January 2022

Published: 18 January 2022

**Publisher's Note:** MDPI stays neutral with regard to jurisdictional claims in published maps and institutional affiliations.



**Copyright:** © 2022 by the authors. Licensee MDPI, Basel, Switzerland. This article is an open access article distributed under the terms and conditions of the Creative Commons Attribution (CC BY) license (<https://creativecommons.org/licenses/by/4.0/>).

## 1. Introduction

When an initially homogeneous solution consisting of at least two chemical species is subjected to a thermal gradient, then mass transfer of the constituents occurs leading to heterogeneity of the solution. This separation effect is known as thermodiffusion or the Soret effect. In addition to the usual expression for the mass flux  $J$  given by Fick's law, an extra part due to the temperature gradient is added, so that

$$J = -\rho D \nabla C - \rho D_T' \nabla T,$$

where  $D$  is the mass diffusion coefficient,  $\rho$  is the density, and  $C$  is the mass fraction of the denser component. Here,  $D_T' = F(C)D_T$  where  $D_T$  is the thermodiffusion coefficient and  $F(C)$  is a particular function of  $C$  satisfying both  $F(C = 0) = 0$  and  $F(C = 1) = 0$ . Most often one uses the function  $F(C) = C(1 - C)$  and, for small variations of the mass fraction  $C$ , it is assumed that  $C(1 - C) \approx C_0(1 - C_0)$ , where  $C_0$  the initial value of the mass fraction. Reviews of heat and mass diffusion in porous media have been performed by Nield and Bejan [1], Ingham and Pop [2], Vasdasz [3] and in the "Handbook of Porous Media" (edited by Vafai) [4]. The Soret effect in liquid mixtures was reviewed by Köhler and Morozov [5]; this seminal paper includes numerous references and deals with thermodiffusion in both the binary and ternary liquid mixtures.

Under the gravity field, the coupling between convection and thermodiffusion, called thermogravitational diffusion, may lead to an important species separation. Thermogravitational separation was studied widely due to its fundamental and (potential) industrial

applications. To name just some industrial applications: the migration of moisture in fibrous insulation, the transport of contaminants in saturated soil, and drying processes or solute transfer in the mushy layer during the solidification of binary alloys.

In 1939, a theory was developed by Furry, Jones and Onsager (FJO) [6]. To obtain the analytical solution of this problem, it was assumed that the term of volumic gravity forces depends only on the temperature  $T$  and not on the mass fraction  $C$ . This is what is called “the hypothesis of the forgotten effect”.

In 1959, Lorenz and Emery [7] considered a thermogravitational column (TGC), consisting of a porous medium, which was saturated by a binary fluid, in order to have a greater thickness of the cell and to obtain a larger quantity of the separated product.

In 1982, Costeseque [8] carried out a basic experimental study on thermodiffusion in porous media, a subject of the doctoral thesis, defended at the University of Toulouse. In 1992, Jamet et al. [9] has presented a modeling approach for the analysis of experimental work, carried out within the framework of Costeseque’s Ph.D. thesis.

After the 2000s, a number of investigations have been carried out, in order either to measure the thermodiffusion coefficients or to increase the species separation in vertical and inclined columns.

Dutrieux et al. [10] reported the two independent techniques used to measure positive Soret coefficients. With one method, the thermodiffusion coefficient,  $D_T$ , was determined by a 5-point sampling process in a TGC. Another method consists of velocity measurements of a transient natural convective state where the velocity measurements are obtained by laser Doppler velocimetry (LDV).

Platten et al. [11] showed that the species separation between the top and the bottom in a TGC can be substantially increased by inclining the column. This result was obtained by experiments performed with a water–ethanol system.

Charrier-Mojtabi et al. [12] presented an analytical and numerical stability analysis of Soret-driven convection in a porous horizontal cavity saturated by a binary fluid. Both the mechanical equilibrium solution and the monocellular flow obtained for particular ranges of the physical parameters of the problem were considered.

Mohammad et al. [13] considered the effect of conducting boundaries on the onset of convection in a porous layer which is heated from below by internal heating. Ouattara et al. [14] studied the effect of conducting boundaries on the onset of convection in a binary fluid-saturated porous horizontal layer. In this study, both analytical and numerical stability analyses were performed. The equilibrium solution was found to lose its stability via either a stationary bifurcation or via a Hopf bifurcation depending on the values of the dimensionless parameters of the problem.

Mojtabi and Rees [15] conducted a theoretical study of the effect of conducting bounding plates on the onset of Horton–Roger–Lapwood convection using both linear and nonlinear stability analyses. Rees and Mojtabi [16] considered the effect of conducting bounding plates on the onset of convection and on the identity of the preferred weakly nonlinear post-critical convection planform. It was shown that convection with a square planform is preferred when the conductivity of the bounding plates is low. Mojtabi et al. [17] presented an analytical and numerical study of species separation in a porous horizontal layer saturated by a binary mixture in the presence of two bounding plates subjected to a constant heat flux. An analytical solution of the unicellular flow which may appear in the cell and realized an optimization of the dimensional separation gradient was developed.

Legros [18] carried out studies in microgravity in order to measure the Soret coefficients in the absence of convective disturbances in Earth gravity. The results were compared with the experimental values obtained on the Earth. Mojtabi [19] presented a new process for the determination of the Soret coefficient of a binary mixture under microgravity.

In the present paper, the influence of the bounding plates on species separation in a vertical TGC is investigated. The objective of this study is to analyze whether the results of the experiments, carried out so far, are sufficiently accurate for the determination of the thermal diffusion coefficients. Indeed, the determination of  $D_T$  from the measurement

of the vertical mass fraction gradient in the TGC used relationships that were obtained without considering the effect of the bounding walls [8,10,11].

### 2. Mathematical Formulation

A parallelepipedic vertical TGC is bounded by vertical and impermeable plates of uniform thickness  $e_s$ . The external surfaces of these plates are maintained at the constant hot and cold temperatures,  $T_h$  and  $T_c$ , respectively; see Figure 1. The horizontal walls ( $y = 0, y = H$ ) are impermeable and insulated. All the boundaries are assumed to be rigid and impermeable. The geometrical dimensions of the cell and the characteristics of the binary mixtures, used in this study, correspond to those considered by Šeta et al. [20].

The thermo-physical characteristics of the walls in [20] are not specified but the characteristics correspond to highly conductive materials. Therefore, three cases (quartz, copper and stainless steel) of wall materials that are found in many experiments [8,10,20] are considered here.

Experimental observations have shown that the flow in TGCs is unicellular. Under these conditions, and whatever the binary fluid considered, the heat transfer within the fluid layer is purely conductive in almost all columns. Once the thickness and the nature of the walls are known, the values of the temperature difference of the internal faces in contact with the binary fluid,  $\Delta T' = T'_h - T'_c$  with  $T'_h < T_h$  and  $T'_c < T_c$  may be deduced. The determination of the thermodiffusion coefficient  $D_T$  using the FJO approach and the measurement of the vertical mass fraction gradient require the knowledge of  $\Delta T'$  and not of the outer temperature difference,  $\Delta T = T_h - T_c$ .

The thermophysical properties of the binary fluid are considered to be constant except for the density in the buoyancy term, which varies linearly with the local temperature  $T$  and the mass fraction  $C$ :

$$\rho = \rho_0[1 - \beta_T(T - T_0) - \beta_C(C - C_0)], \tag{1}$$

where  $\beta_T$  and  $\beta_C$  are the thermal and mass expansion coefficients of the binary fluid, respectively, and both the temperature,  $T_0$ , and the concentration,  $C_0$ , correspond to the reference state. The value  $\rho_0$  is the fluid mixture reference density at  $T = T_0$  and  $C = C_0$ . Under these conditions, the governing conservation equations for mass, momentum, energy and chemical species for the bulk read:

$$\left\{ \begin{array}{l} \nabla \cdot \mathbf{V} = 0, \\ \left[ \frac{\partial \mathbf{V}}{\partial t} + (\mathbf{V} \cdot \nabla) \mathbf{V} \right] = -\frac{\nabla P}{\rho_0} - [1 - \beta_T(T_2 - T_0) - \beta_C(C - C_0)]g\mathbf{y} + \nu \nabla^2 \nabla, \\ \frac{\partial T_2}{\partial t} + \mathbf{V} \cdot \nabla T_2 = \nabla \cdot (a \nabla T_2), \\ \frac{\partial C}{\partial t} + \mathbf{V} \cdot \nabla C = \nabla \cdot [D \nabla C + D_T C_0 (1 - C_0) \nabla T_2], \end{array} \right. \tag{2}$$

where  $V$  is the fluid velocity,  $T_2$  is the temperature inside the bulk,  $\nu$  is the kinematic viscosity, and  $a$  is the thermal diffusivity. For the two plates bounding the bulk, the conduction heat transfer equations read:

$$\left\{ \begin{array}{l} \frac{\partial T_1}{\partial t} = a_s \nabla^2 T_1, \\ \frac{\partial T_3}{\partial t} = a_s \nabla^2 T_3, \end{array} \right. \tag{3}$$

where  $T_1$  and  $T_3$  are the temperatures within the two vertical plates, respectively, and  $a_s$  their common thermal diffusivities. Thus, it is assumed that the bounding plates are made from the same material and are also of equal thickness,  $e_s$ .

By considering the continuity of the temperatures and the heat fluxes at the solid/porous interfaces,  $x = 0$  and  $x = e_f$ , the full set of dimensionless boundary and interface conditions become:

$$\left\{ \begin{array}{l} x = -e_s, T_1 = T_h, \\ x = 0, T_1 = T_2, \frac{\partial T_1}{\partial x} = \frac{1}{d} \frac{\partial T_2}{\partial x}, \\ x = e_f, T_2 = T_3, \frac{\partial T_3}{\partial x} = \frac{1}{d} \frac{\partial T_2}{\partial x}, \\ x = e_f + e_s, T_3 = T_c, \end{array} \right. \quad (4)$$

where  $d = \lambda_s/\lambda_f$  is the thermal conductivity ratio of the solid bounding plates and the binary fluid. The binary fluid velocity field verifies:

$$\forall M \in \partial\Omega, \mathbf{V} = 0, \quad (5)$$

where  $\partial\Omega$  denotes the solid part delimiting the binary fluid and  $\Omega$  is the volume, occupied by the fluid; see Figure 1.

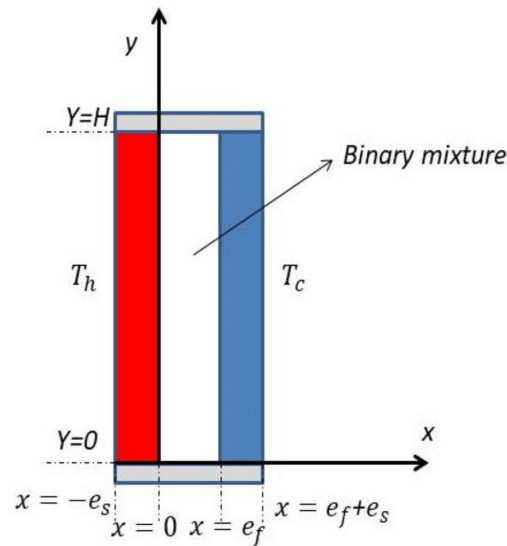


**Figure 1.** Geometrical configuration of the vertical thermogravitational column (TGC). See text for details.

### 3. Analytical Solution of the Unicellular Flow

#### 3.1. Analytical Solution of the Thermal and Dynamic Field in the TGC

For the limiting case of a narrow cavity,  $H \gg e_f$ , we considered the parallel flow approximation which is often used (see, e.g., [15]) to determine the velocity and the temperature and mass fraction fields. For this analytical study, it is assumed here that the temperature fields,  $T_1, T_2, T_3$ , within the two solid walls and in the fluid do not depend on the variable  $y$  in a large part of the vertical column except for the immediate neighborhoods of  $y = 0$  and  $y = H$ . This hypothesis is justified by the numerical simulations carried out in this study. The stationary 2-dimensional unicellular flow is then given as follows:

$$\mathbf{V} = W(x)\mathbf{y}, \quad T_2 = f_2(x), \quad C = my + h(x), \quad T_1 = f_1(x), T_3 = f_3(x), \quad (6)$$

where  $\vec{V}$  has only the component  $W(x)\mathbf{y}$  except in the vicinity of the lower and upper boundaries. The functions  $W(x)$  and  $f_i(x), i = 1, 2, 3$ , depend solely on the  $x$ -component, and  $m$  is a yet-unknown constant, representing the mass fraction gradient in the  $y$ -direction.

With the above-made assumptions and for the steady state, the system (3) and the heat transport equation for the binary fluid are reduced to the following set of equations:

$$\begin{cases} \frac{\partial^2 f_1}{\partial x^2} = 0, \\ \frac{\partial^2 f_2}{\partial x^2} = 0, \\ \frac{\partial^2 f_3}{\partial x^2} = 0. \end{cases} \tag{7}$$

Using the boundary conditions (4), one obtains the following expressions for the temperature fields in the two solid walls and in the fluid layer:

$$\begin{cases} T_1 = \left( -(T_h - T_c)x + (T_h + T_c)e_s + T_h de_f \right) / (de_f + 2e_s), \\ T_2 = \left( -(T_h - T_c)xd + (T_h + T_c)e_s + T_h de_f \right) / (de_f + 2e_s), \\ T_3 = \left( -(T_h - T_c)x + (T_h + T_c)e_s + ((d - 1)T_c + T_h)e_f + T_h de_f \right) / (de_f + 2e_s). \end{cases} \tag{8}$$

The temperature drop between the different faces of the TGC then is:

$$\begin{aligned} \Delta T_1 &= \frac{(T_h - T_c)e_s}{de_f + 2e_s} = T_1(x = -e_s) - T_1(x = 0) = T_h - T'_h, \\ \Delta T_2 &= \frac{(T_h - T_c)de_f}{de_f + 2e_s} = T_2(x = 0) - T_2(x = e_f) = T'_h - T'_c, \\ \Delta T_3 &= \frac{(T_h - T_c)e_s}{de_f + 2e_s} = T_3(x = e_f) - T_2(x = e_f + e_s) = T'_c - T_c. \end{aligned} \tag{9}$$

These temperature drops across the column may also be expressed in terms of thermal resistance ratios of the solid walls,  $R_s = e_s / \lambda_s$ , of the fluid layer,  $R_f = e_f / \lambda_f$ , and of the total thermal resistance of the TGC,  $R_t = 2e_s / \lambda_s + e_f / \lambda_f$ , where the expressions  $\frac{e_s}{de_f + 2e_s} = R_s / R_t$  and  $\frac{de_f}{de_f + 2e_s} = R_f / R_t$  denote thermal resistance ratios.

From the above, one finds:

$$\Delta T' = T'_h - T'_c = \left( \frac{R_f}{R_t} \right) (T_h - T_c) = \left( \frac{R_f}{R_t} \right) \Delta T. \tag{10}$$

The temperature difference  $\Delta T'$ , felt directly by the binary fluid, verifies that  $\Delta T' \ll \Delta T$  if the thermal resistance ratio satisfies  $R_f / R_t \ll 1$  condition. The resistance,  $R_s$ , increases as the wall thickness increases and as the thermal conductivity decreases.

By considering the results on the temperature field in the TGC, the system (2) reduces to:

$$\begin{cases} P = P(z), \\ g(\beta_T \frac{\partial T_2}{\partial x} + \beta_C \frac{\partial h}{\partial x}) + \nu \frac{\partial^3 W}{\partial x^3} = 0, \\ mW(x) = D \frac{\partial^2 h}{\partial x^2}. \end{cases} \tag{11}$$

In 1939, Furry, Jones, and Onsager [6] established the conservation equations of the balance sheet to describe the thermal gravitational diffusion process for a binary mixture of gas confined within a differentially heated, vertical rectangular cavity. However, in this study, the role of the mass fraction in the gravity force term was ignored because the temperature field was considered to establish itself in the enclosure faster than the mass fraction field was doing. This hypothesis is often called “the forgotten effect”. The Navier–Stokes equation then becomes:

$$g\beta_T \frac{\partial T_2}{\partial x} + \nu \frac{\partial^3 W}{\partial x^3} = 0. \tag{12}$$

By replacing  $\frac{\partial T_2}{\partial x}$  with its value,  $-\frac{(T_h - T_c)d}{de_f + 2e_s} = -\Delta T'$ , in Equation (11), and considering that the mass flow through each horizontal section of the cavity satisfies the zero-vertical-

flux condition:  $\int_0^{e_f} W dx = 0$ , one obtains the solution of the differential equation (11) once the boundary conditions are taken into account:

$$W = -\frac{g\beta_T\Delta T'x(e_f - x)(2x - e_f)}{12ve_f} \tag{13}$$

Note that as soon as one takes into account the influence of the walls, the fluid velocity is slightly lower than when the temperature drop is not taken into account:  $W/W_0 = \Delta T' / \Delta T = \frac{de_f}{de_f + 2e_s}$ , where  $W_0$  corresponds to the velocity  $W$  when the influence of the walls is absent.

If this velocity is put in dimensionless form by using the velocity scale based on the thermal diffusivity of the binary mixture ( $\alpha/e_f$ ) with the thickness,  $e_f$ , of the column as the length scale, the following non-dimensional expression of the velocity is obtained:

$$\bar{W} = -\frac{Ra_T\bar{x}(1 - \bar{x})(2\bar{x} - 1)}{12} \tag{14}$$

where  $\bar{W}$ ,  $\bar{x}$  are the velocity and the non-dimensional coordinate, respectively, and  $Ra_T$  is the thermal Rayleigh number. The intensity of the vertical velocity is therefore proportional to the thermal Rayleigh number.

### 3.2. Analytical Solution of the Mass Fraction Field in the TGC

By replacing  $W(x)$  with its expression given in the last equation of system (13), one obtains:

$$h(x) = -\frac{mg\beta_T\Delta T'}{12ve_fD} \left( \frac{x^5}{10} - \frac{e_f x^4}{4} + \frac{e_f^2 x^3}{6} \right) + n_1 x + n_2 \tag{15}$$

The expression (15) contains three constants ( $m, n_1, n_2$ ) to be determined, in order to obtain an expression for the mass fraction field  $C$  in the TGC. These three constants may be found by applying the following three conditions:

1. Zero mass flux on one of the vertical walls,  $J_{x=0} = 0$ .
2. Mass flow through any horizontal section is zero once the stationary states have reached:  $\int_0^{e_f} (WC - D\frac{\partial C}{\partial x}) dx = 0$ .
3. Each component in the TGC is assumed to be conserved,  $\int_0^H dy \int_0^{e_f} C dx = C_0 H e_f$ .

Then, the expressions for the constants  $n_1$  and  $n_2$  read:

$$n_1 = -\frac{D_T C_0 (1 - C_0) \Delta T'}{D e_f}, \quad n_2 = \frac{mg\beta_T\Delta T'e_f^4 + 720v(D(2C_0 - mH) + D_T C_0(1 - C_0)\Delta T')}{1440Dv}$$

and the mass fraction gradient is:

$$m = \frac{504g\beta_T v \Delta T'^2 e_f^2 D_T C_0 (1 - C_0)}{(g\beta_T \Delta T' e_f^3)^2 + 362880(Dv)^2} \tag{16}$$

The mass fraction gradient now depends on the characteristics of the binary fluid being studied ( $D_T, D, v, \beta_T$ ), on the thickness,  $e_f$ , and on the imposed thermal gradient,  $\Delta T'$ . Thus,  $m$  does not admit an extremum according to the two parameters ( $e_f, \Delta T'$ ). Indeed, the system,

$$\left\{ \frac{\partial m}{\partial e_f} = 0, \frac{\partial m}{\partial \Delta T'} = 0 \right\} \tag{17}$$

admits only solutions  $\{e_f = 0, \Delta T'\}$  and  $\{e_f, \Delta T' = 0\}$ . On the other hand, for  $\Delta T'$  fixed, one obtains:

$$e_{opt} = 2(2835)^{1/6} (Dv/g\beta_T\Delta T')^{1/3} \tag{18}$$

and for a fixed  $e_f$  there is a trivial solution,  $\Delta T' = 0$ , given the minimum and maximum values of  $m$ , independent of  $\Delta T'$ , which is quickly reached for a low value of  $\Delta T'$ ; see Figure 2.

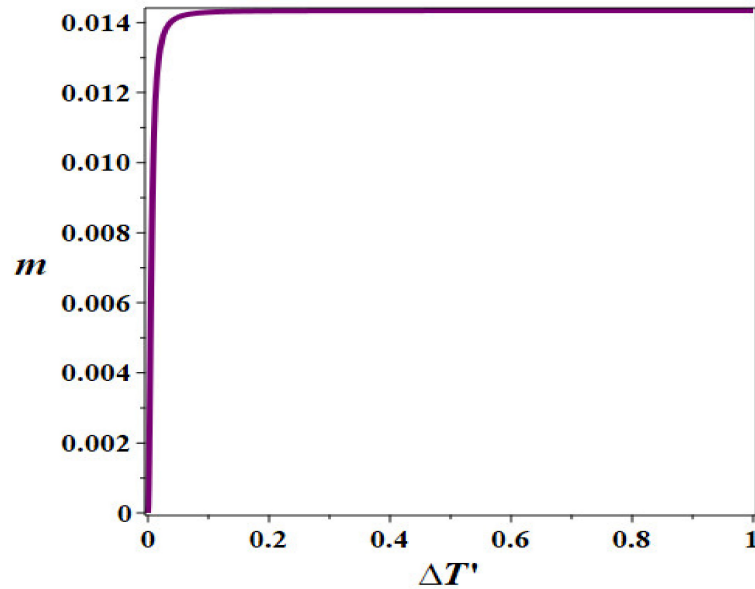


**Figure 2.** Variation of the mass fraction gradient  $m$  according to the temperature difference  $\Delta T'$  for the binary solution toluene methanol and the thickness  $e_f = 10^{-3}$  mm.

From the optimal thickness  $e_{opt}$ , one obtains the optimal mass fraction gradient:

$$m_{opt} = \frac{105^{1/3}(D\nu g^2 \beta_T^2 D \Delta T'^2)^{2/3} D_T C_0 (1 - C_0)}{90 g \nu g \beta_T D^2} \tag{19}$$

Equation (16) leads to an expression for the thermodiffusion coefficient  $D_T$  of the present binary mixture:

$$D_T = \frac{m(g\beta_T \Delta T' e_f^3)^2 + 362880(D\nu)^2}{504g\beta_T \nu \Delta T'^2 e_f^2 C_0 (1 - C_0)} \tag{20}$$

Equation (20) shows that the value of the thermodiffusion coefficient,  $D_T$ , obtained from the measurement of the vertical mass fraction gradient,  $m$ , depends not only on  $\Delta T$  but also on the temperature difference of the internal faces that are in contact with the binary fluid.

For the different mixtures of binary solutions studied, the second term,  $362880(D\nu)^2$  of the denominator of Equation (16) is negligible compared with the first term,  $(g\beta_T \Delta T' e_f^3)^2$ . In the case of the binary water (60.88 wt%)–ethanol (39.12 wt%) mixture at a mean temperature of 22.5 °C, the second term,  $362880(D\nu)^2 = 4.995627615 \cdot 10^{-25}$ , which is much smaller than the first term,  $(g\beta_T \Delta T' e_f^3)^2 = 5.945427764 \cdot 10^{-21}$ . Similar results are found here for the two binary solutions studied by Šeta et al. [20]. In this case, one obtains a simplified form for the mass fraction gradient to replace Equation (16):

$$m_{simpl} \approx \frac{504\nu D_T C_0 (1 - C_0)}{g\beta_T e_f^4} \tag{21}$$

Under these conditions  $m_{simpl}$  does not depend on  $\Delta T'$ , anymore what agrees with the experimental results for binary solutions.



The full expression for the mass fraction gradient  $m$  depends on  $\Delta T'$  in the case of binary *gas* mixtures. Indeed, for several varieties of binary gas mixtures, such as (He, CO<sub>2</sub>) and (He, N<sub>2</sub>), it is the second term in the denominator of Equation (16), namely  $362880(D\nu)^2$ , which dominates the first term,  $(g\beta_T\Delta T'e_f^3)^2$ . It follows, therefore, that Equation (16) may only be used for the determination of the thermodiffusion coefficient for binary gas mixtures. The physical interpretation of this result can be summarized as follows: the importance of species separation in TGC depends on the good match between the physical time associated with the flow velocity and the mass diffusion time. For example, some experimenters have used porous TGC [7,9] to reduce the velocity of convective flow.

Equation (13) shows that the velocity  $W$  in TGC is proportional to  $\frac{\beta_T\Delta T}{\nu}$ . The kinematic diffusivity of liquids is of the same order of magnitude as the one for gases (it is the case of water and air). On the other hand, the thermal expansion coefficient of gases is two orders of magnitude greater than that for liquids. It follows that, within the same TGC subjected to the same temperature difference, the convective velocity in the binary gas mixture is much greater than the velocity in the liquid mixture. A modification of the temperature difference imposed on the column therefore leads to a greater variation in the mass fraction in the case of gas mixtures compared to the one in liquid mixtures.

In vertical TGCs, the species separation of a binary mixture,  $\Delta C$ , is defined by the difference between the mass fraction at the bottom of the column,  $C_b$  and at the top of the column,  $C_t$ , for a positive separation factor  $D_T$ :

$$\Delta C = C_b - C_t = mH. \quad (22)$$

The analytical and numerical results obtained in this study can be illustrated by restricting ourselves to the experimental values of the thermophysical parameters of the toluene (18.9 wt%)–methanol (81.1 wt%) mix [20]. The values of the thermophysical properties of the two binary mixtures at the average temperature  $T = 22$  °C are given in Table 1.

**Table 1.** Properties for toluene–methanol mixtures at a mean temperature of 23 °C and  $C_0 = 18.9$  wt%. See text for details.

$D[\text{m}^2\text{s}^{-1}]$	$D_T[\text{m}^2\text{s}^{-1}\text{K}^{-1}]$	$\beta_c$	$\beta_T[\text{K}^{-1}]$	$\alpha[\text{m}^2\text{s}^{-1}]$	$\rho_0[\text{kg}\cdot\text{m}^{-3}]$	$\nu[\text{m}^2\text{s}^{-1}]$
$2.49 \times 10^{-9}$	$8.6 \times 10^{-12}$	0.00923	$1.189 \times 10^{-3}$	$1.029 \times 10^{-7}$	800.495	$7.02 \times 10^{-7}$

Figure 3 shows the variation of the species separation as a function of the thickness of the vertical toluene–methanol layer of height  $H = 30$  mm and for the temperature difference  $\Delta T' = 6$  °C, a configuration which is similar to that studied by Šeta et al. [20].

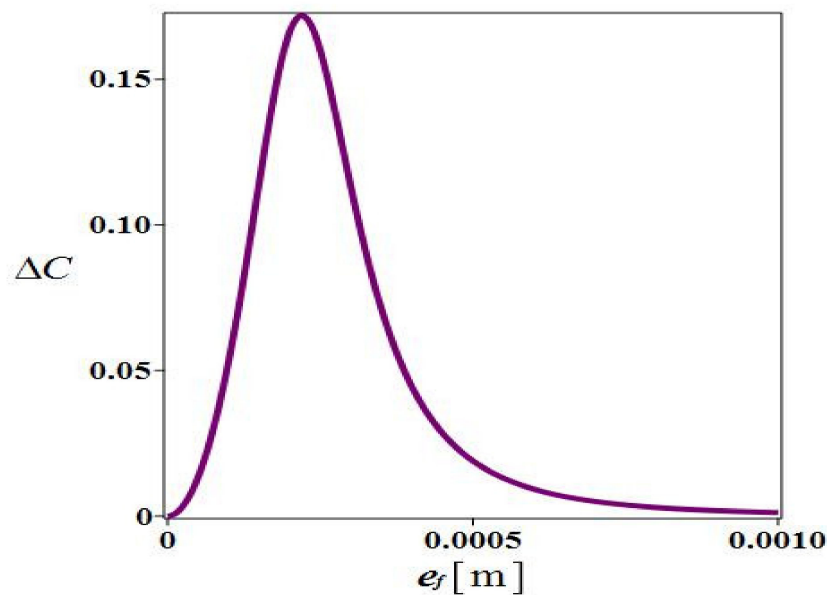


**Figure 3.** Variation of the species separation dependence on the thickness  $e_f$  of the toluene–methanol layer of height  $H = 30$  mm, the initial value of the mass fraction  $C_0 = 18.9$  wt%, and  $\Delta T' = 6$  °C.

#### 4. Comparisons between Analytical and Numerical Calculations

##### 4.1. Dimensional Numerical Simulation

The dimensional sets of equations and boundary conditions obtained from systems (2) and (3) were solved numerically using the commercial finite element code, COMSOL Multiphysics [21], with a uniform rectangular mesh. The time-dependent solver and the set of equations (incompressible Navier–Stokes, thermal and mass diffusion equations) in transient form were used. The condition of conservation of the average mass fraction in the cavity was imposed on each of the iterations. Direct numerical simulations were then performed for vertical thermogravitational column with the dimensions,  $H = 30$  mm,  $e_f = 0.5$  mm and  $e_s = 1$  and 2 mm.

The rectangular spatial resolutions were used: 15–200 up to 20–300 for the solid plates and 25–200 up to 30–300 for the fluid domain. The passage, in the fluid column of thickness  $e_f$  and height  $H$ , from the quadrangle mesh 30–300 to a finer mesh 40–400, gives the same results.

##### 4.2. Consideration of the Characteristics of the Walls on the Temperature Field in a TGC

For the analytical model, developed in this study, it is assumed that the height,  $H$ , of the TGC is much larger than the thickness of the binary fluid layer,  $e_f$ . Due to the reversal of the fluid flow at the horizontal walls  $y = 0$  and  $y = H$ , this theoretical model does not allow us accessing the temperature of the binary fluid in the vicinity of  $y = 0$  and  $y = H$ .

- a. Temperature as a function of  $x$  for  $y = 15$  mm in a TGC with  $e_s = 1$  mm and  $e_f = 0.5$  mm.

Figure 4 shows that the heat transfer on almost the entire central part of the TGC is purely conductive within the binary fluid.

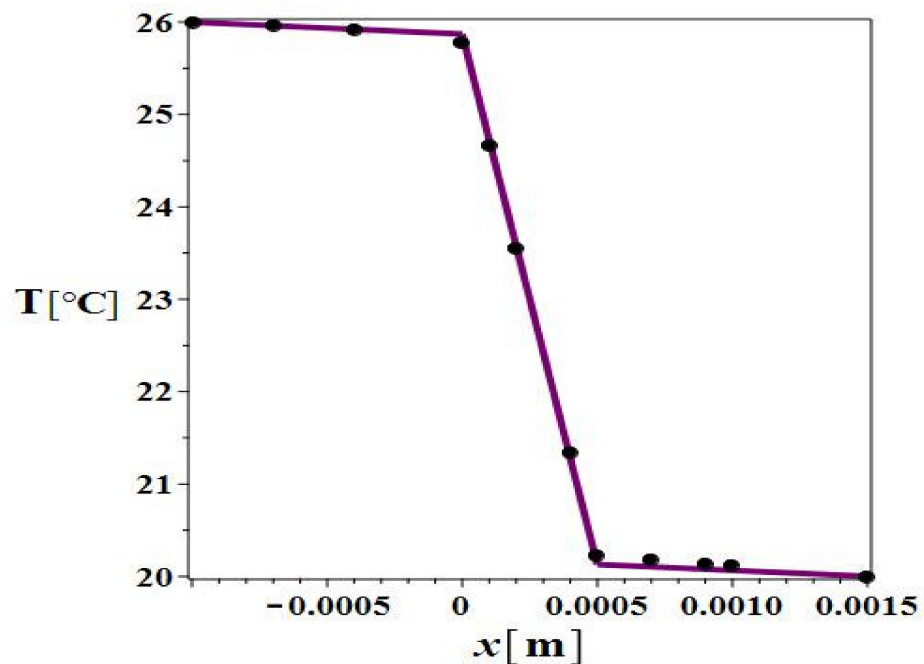


**Figure 4.** Temperature variation as a function of  $x$  for  $y = 15$  mm in the TGC which is maintained at  $T_h = 26^\circ\text{C}$ ,  $T_c = 20^\circ\text{C}$  and containing the binary fluid toluene–methanol. Numerical calculations are shown by black dots and analytical results are given by red line.

b. Temperature as a function of  $y$  for  $x = 0$  and  $x = e_f = 0.5$  mm.

The results of direct numerical simulation show (Figure 5) that the temperature at the level of the binary solid–fluid interface ( $x = 0$ ) is not isothermal in the vicinity of the two horizontal surfaces  $y = 0$  and  $y = 0.03$  m.

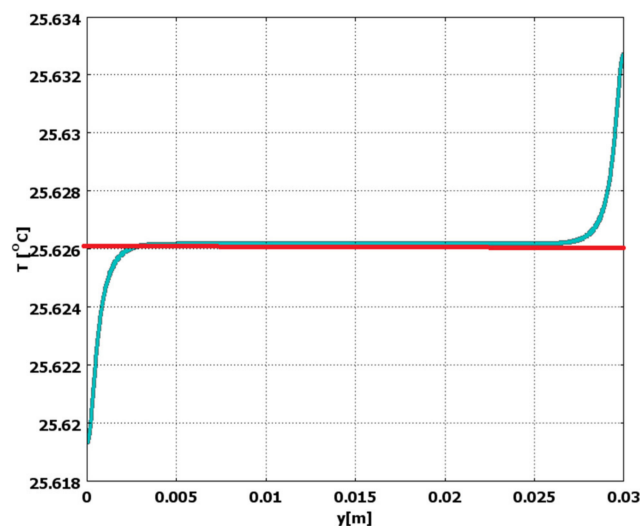


**Figure 5.** Temperature at the solid interface, for a toluene–methanol binary fluid at  $x = 0$ . The analytical solution is shown in red and the numerical calculations are given in green.

The results of direct numerical simulation show (Figure 6) that the temperature at the level of the binary solid–fluid interface ( $x = 5 \cdot 10^{-4}$  m) is not isothermal in the vicinity of the two horizontal surfaces  $y = 0$  and  $y = 0.03$  m

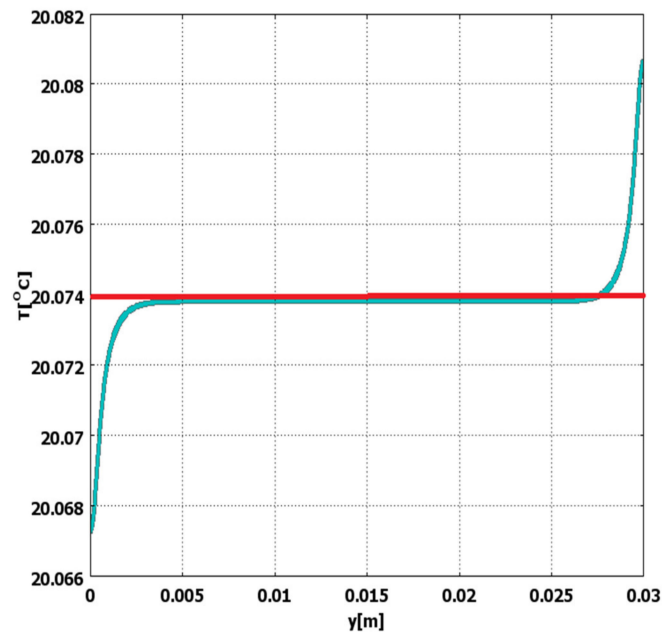


**Figure 6.** Temperature at the solid interface for a toluene–methanol binary fluid at  $x = e_f = 5 \cdot 10^{-4}$  m. The analytical solution is given in red and the numerical calculation is shown in green.

4.3. Mass Fraction Field in a TGC

4.3.1. Mass Fraction Field without Consideration of the Walls

When the influence of the walls is not taken into account, it must be noted that the numerical and analytical results obtained here are in good agreement. In Table 2, the numerical and analytical results, calculated here from  $m$  and  $m_{simpl}$ , are compared to those, obtained by Šeta et al. [20] for a TGC of height  $H = 30$  mm and thickness  $e_f = 0.5$  mm. The numerical and theoretical solutions for  $\Delta T = 6$  °C and  $\Delta T = 10$  °C lead to  $\Delta C = 0.0152$  are in good agreement. However, the findings in [20] lead to  $\Delta C = 0.0142$ . The differences between the results of the current study and those of Šeta et al. [20] for  $\Delta T = 10$  °C are partly due to the fact that the current calculations are given with four decimals while those of [20] are performed with three decimals.

**Table 2.** Mass fraction values,  $C(x = 0.25$  mm,  $y = (3, 27)$  mm), obtained at the steady state, in the vertical TGC with toluene–methanol mixtures, for  $T_h = 26$  °C,  $T_c = 20$  °C and for  $T_h = 28$  °C,  $T_c = 18$  °C.

$\Delta T$ °C	C	Ref. [20]	Numerical Results	Analytical Results	
				$m$ [m <sup>-1</sup> ]	$m_{simpl}$ [m <sup>-1</sup> ]
6	$C_{y=0.003}$	0.1964	0.1965	0.1961	0.1962
6	$C_{y=0.027}$	0.1818	0.1813	0.1809	0.1808
10	$C_{y=0.003}$	0.196	0.1967	0.1958	0.1959
10	$C_{y=0.027}$	0.182	0.1813	0.1806	0.1805

4.3.2. Mass Fraction Field with Consideration of the Wall Characteristics

The walls used in TGCs are usually made of copper or stainless steel [8,10,11] to avoid corrosion problems; in Šeta et al. [20], quartz walls were used.

When the plates are made of stainless steel 1 mm thick, the values of the temperatures at the interfaces bounding the binary mixture namely,  $\Delta T' = 5.7$  °C and  $9.5$  °C, are very close to the temperatures which are applied to the exterior walls,  $\Delta T = 6$  °C and  $10$  °C, respectively. However, in the case of the quartz walls, used by Šeta et al. [20], the difference between  $\Delta T'$  and  $\Delta T$  for each interface is more important:  $\Delta T' = 8.4$  °C, for  $\Delta T = 10$  °C and  $e_s = 2$  mm. As indicated in Table 2, the differences between the values of

$C$  obtained analytically by taking into account the characteristics of the walls and those obtained without taking them into account are very small. This result is in accordance with theoretical considerations (Equation (21)), indicating that in the case of binary solutions, the mass fraction gradient is independent of the temperature difference applied to the thermogravitational columns.

On the other hand, considering the characteristics of the walls for a TGC with  $H = 30$  mm and  $\Delta T = 6$  °C, the numerical simulations provide less important species separation,  $\Delta C = 0.010$ , compared to the analytical result,  $\Delta C = 0.019$ . For the TGC with the same geometrical and physical characteristics but with a height 10 times as large,  $H = 300$  mm, numerically  $\Delta C = 0.102$  and analytically  $\Delta C = 0.19$  are found. These results show that the species separation is proportional to the height of the TGC.

The plot of the mass fraction  $C$  as a function of  $y$  for  $x = 0.25$  mm (Figure 7), for  $\Delta T = 6$  and  $H = 30$  mm, obtained at the steady state, in the vertical TGC with a toluene/methanol mixture, shows good agreement between the analytical calculations (red line) and the direct numerical simulation results (black dots) in the central part of the TGC.

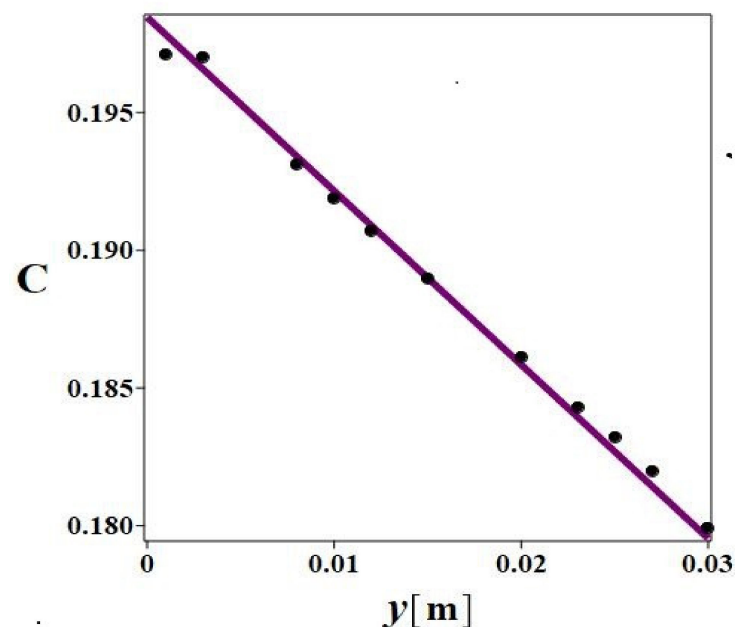


**Figure 7.** Mass fraction values,  $C(x = 2.5 \cdot 10^{-4}$  m) as a function of height  $y$ , for toluene–methanol binary fluid. Analytical solution is shown by red line and numerical calculations are given by black dots.

In order to explain the slight difference between the numerical and analytical results on species separation, the steam function, the iso-mass fraction lines and mass fraction field are plotted for the upper (Figure 8a) and for the lower (Figure 8b) parts of TGC. Figure 8c presents the thermal field inside the TGC and its bounding plates, in its lower part and the steam function in the binary fluid slot, in the case of toluene–methanol with  $\Delta T = 6$  °C ( $T_h = 26$  °C,  $T_c = 20$  °C)

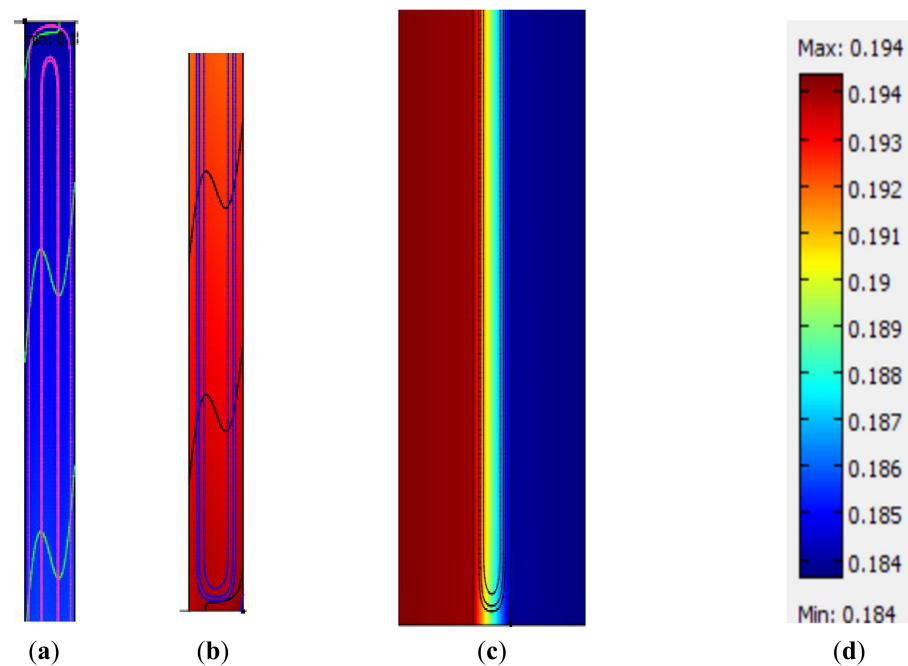


**Figure 8.** Stream function, the iso-mass fraction lines and mass fraction field: upper (a) and lower (b) parts of the TGC and inside the binary fluid. (c) Thermal field in the cell and the bounding plates, in the lower part of the TGC and streamlines inside the binary fluid toluene–methanol. (d) Mass fraction field scale.  $\Delta T = 6\text{ }^{\circ}\text{C}$  ( $T_h = 26\text{ }^{\circ}\text{C}$ ,  $T_c = 20\text{ }^{\circ}\text{C}$ ).

As one can see from Figure 8a,b, giving the mass fraction field scale presented in Figure 8d, the mass fraction  $C$  is around 0.180 at the upper part of the cavity and around 0.198 at its lower part. These results agree with those, shown in Figure 7. However, at the vicinity of the horizontal walls, the velocity of the binary fluid is very weak, which is not a condition used for the determination of the analytical solution (parallel flow approximation).

## 5. Conclusions

In this paper, the theory of Furry, Jones and Onsager (FJO) [6] is extended to the cases where bounding conducting walls encircle the thermogravitational column (TGC), a situation which will arise necessarily in experimental work, and for which the influence of the characteristics of the walls delimiting the TGC was not considered earlier. A study of the influence of the thickness and of the thermal properties of the bounding plates on the species separation in a TGC is presented here.

An analytical solution is developed under the hypotheses of the “forgotten effect” and the parallel flow approximation. The temperature distribution within the binary fluid and the two bounding plates is determined, as well as the velocity and the mass fraction fields within the binary fluid. The direct numerical simulations, without these two hypotheses, led to almost identical analytical results outside the immediate vicinity of the horizontal walls of the TGC.

By using the expression for the vertical mass fraction gradient,  $m$ , obtained, it is found that the magnitude of the thermodiffusion coefficient depends on  $\Delta T' = T'_h - T'_c$ , i.e., on the temperature difference across the binary fluid layer rather than across the TGC itself. However, for most experiments, performed with binary liquids solutions,  $m$  is replaced by  $m_{simpl}$  which does not depend on the temperature difference.

So, for binary liquids, the theory of FJO predicts that the species separation is independent of the temperature difference  $\Delta T = T_h - T_c$ . This result is also corroborated numerically and analytically by analyzing the species separation in a column without considering the influence of the walls. It is also observed that for gas mixtures, this result is

no longer valid., i.e., the vertical mass fraction gradient does depend on the temperature difference.

The obtained analytical results, based on a TGC of infinite vertical extension, and the numerical results, which did not consider the thickness of the walls, are found to be in good agreement with the results obtained numerically and experimentally by Šeta et al. [20]. However, when the thermophysical characteristics of the walls delimiting the TGC of finite height are taken into account in the numerical simulations, a slightly weaker species separation is found compared to the analytical results, obtained in the case where the TGC was assumed to have infinite vertical extension.

**Author Contributions:** Conceptualization, A.M.; methodology, software, validation, writing, A.M., P.C., B.O., M.-C.C.-M., D.A.S.R. All authors have read and agreed to the published version of the manuscript.

**Funding:** This research received no external funding.

**Data Availability Statement:** Not applicable.

**Acknowledgments:** This work was supported by CNES, the French National Space Agency.

**Conflicts of Interest:** The authors declare no conflict of interest.

## References

1. Nield, D.A.; Bejan, A. *Convection in Porous Media*; Springer: New York, NY, USA, 2013. [CrossRef]
2. Ingham, D.B.; Pop, I. (Eds.) *Transport Phenomena in Porous Media*; Pergamon/Elsevier Science: Oxford, UK, 1998; pp. 155–178. [CrossRef]
3. Vadász, P. (Ed.) *Emerging Topics in Heat and Mass Transfer in Porous Media*; Springer Science+Business Media B.V.: Dordrecht, The Netherlands, 2008. [CrossRef]
4. Vafai, K. (Ed.) *Handbook of Porous Media*; Taylor & Francis Group/CRC Press: Boca Raton, FL, USA, 2005; pp. 269–320. [CrossRef]
5. Köhler, W.; Morozov, K.I. The Soret effect in liquid mixtures—A review. *J. Non-Equilib. Thermodyn.* **2016**, *41*, 151–197. [CrossRef]
6. Furry, W.H.; Jones, R.C.; Onsager, L. On the theory of isotope separation by thermal diffusion. *Phys. Rev.* **1939**, *55*, 1083–1095. [CrossRef]
7. Lorenz, M.; Emery, A. The packed thermal diffusion column. *Chem. Eng. Sci.* **1959**, *11*, 16–23. [CrossRef]
8. Costesèque, P. On Selective Migration of Isotopes and Elements by Thermodiffusion in Aqueous Solutions. Applications of the Thermogravitational Effect in Porous Media; Experimental Observations and Geochemical Consequences. Ph.D. Thesis, Université Paul Sabatier Toulouse, Toulouse, France, 1982.
9. Jamet, P.; Fargue, D.; Costesèque, P.; De Marsily, G.; Cernes, A. The thermogravitational effect in porous media: A modelling approach. *Transp. Porous Media* **1992**, *9*, 223–240. [CrossRef]
10. Dutrieux, J.F.; Platten, J.K.; Chavpeyer, G.; Bou-Ali, M.M. On the measurement of positive Soret coefficients. *J. Phys. Chem. B* **2002**, *106*, 6104–6114. [CrossRef]
11. Platten, J.K.; Bou-Ali, M.M.; Dutrieux, J.F. Enhanced molecular separation in inclined thermogravitational columns. *J. Phys. Chem. B* **2003**, *107*, 11763–11767. [CrossRef]
12. Charrier-Mojtabi, M.C.; Elhajjar, B.; Mojtabi, A. Analytical and numerical stability analysis of Soret-driven convection in a horizontal porous layer. *Phys. Fluids* **2007**, *19*, 124104. [CrossRef]
13. Mohammad, A.N.; Rees, D.A.S.; Mojtabi, A. The effect of conducting boundaries on the onset of convection in a porous layer which is heated from below by internal heating. *Transp. Porous Media* **2017**, *117*, 189–206. [CrossRef]
14. Ouattara, B.; Khouzam, A.; Mojtabi, A.; Charrier-Mojtabi, M.C. Analytical and numerical stability analysis of Soret-driven convection in a horizontal porous layer: The effect of conducting bounding plates. *Fluid Dyn. Res.* **2012**, *44*, 031415. [CrossRef]
15. Mojtabi, A.; Rees, D.A.S. The effect of conducting bounding plates on the onset of Horton–Rogers–Lapwood convection. *Int. J. Heat Mass Transf.* **2011**, *54*, 293–301. [CrossRef]
16. Rees, D.A.S.; Mojtabi, A. The effect of conducting boundaries on weakly nonlinear Darcy–Bénard convection. *Transp. Porous Media* **2011**, *88*, 45–63. [CrossRef]
17. Mojtabi, A.; Ouattara, B.; Rees, D.A.S.; Charrier-Mojtabi, M.-C. The effect of conducting bounding horizontal plates on species separation in porous cavity saturated by a binary mixture. *Int. J. Heat Mass Transf.* **2018**, *126*, 479–488. [CrossRef]
18. Legros, J. Double diffusive instabilities and the Soret coefficient measurement under microgravity conditions. *Acta Astronaut.* **1987**, *15*, 455–461. [CrossRef]
19. Mojtabi, A. A new process for the determination of the Soret coefficient of a binary mixture under microgravity. *Int. J. Therm. Sci.* **2019**, *149*, 106204. [CrossRef]

- 
20. Šeta, B.; Lapeira, E.; Dubert, D.; Gavalda, F.; Bou-Ali, M.M.; Ruiz, X. Separation under thermogravitational effects in binary mixtures. *Eur. Phys. J. E* **2019**, *42*, 58. [[CrossRef](#)] [[PubMed](#)]
  21. COMSOL Multiphysics Simulation Software. Available online: <https://www.comsol.com/comsol-multiphysics> (accessed on 5 January 2022).